Center for Turbulence Research
Proceedings of the Summer Program 1988

Inflow/Outflow Boundary Conditions and Global Dynamics of Spatial Mixing Layers

By J. C. Buell[1] AND P. Huerre[2]

1. Introduction

The numerical simulation of incompressible spatially-developing shear flows poses a special challenge to computational fluid dynamicists. The Navier-Stokes equations are elliptic and boundary equations need to be specified at the inflow and outflow boundaries in order to compute the fluid properties within the region of interest. It is, however, difficult to choose inflow and outflow conditions corresponding to a given experimental situation. Furthermore the effects that changes in the boundary conditions or in the size of the computational domain may induce on the global dynamics of the flow are presently unknown. The purpose of this study is to examine these issues in light of recent developments in hydrodynamic stability theory. The particular flow to be considered is the spatial mixing layer but it is expected that similar phenomena are bound to occur in other cases such as channel flow, the boundary layer, etc. A short summary of local/global and absolute/convective instability concepts is given in section 2. In section 3 we present the results of numerical simulations which strongly suggest that global resonances may be triggered in domains of finite streamwise extent although the evolution of the perturbation vorticity field is everywhere locally convective. In the last section, we discuss a relationship between finite domains and pressure sources which might help in devising a scheme to eliminate these difficulties.

2. Local/Global, Absolute/Convective Instabilities

Rigorous definitions of absolute and convective instability have been given in the context of plasma physics by Briggs (1964) and Bers (1983). Similar ideas have recently been applied to inviscid instabilities in free shear layers by Huerre & Monkewitz (1985), Koch (1985) and Monkewitz (1988), among others. For a review, the reader is referred to Huerre (1987).

A parallel flow (*i.e.*, independent of the streamwise coordinate x) is said to be convectively unstable if its linear response to a delta function impulse in space and time decays to zero everywhere as time increases to infinity, but increases along certain rays in the downstream direction (Figure 1b). Conversely, a parallel flow is absolutely unstable if its impulse response becomes unbounded everywhere for infinite time (Figure 1a). These notions are particularly relevant in spatially-evolving flows, as long as the streamwise variations of the basic velocity profile are

1 NASA Ames Research Center

2 Department of Aerospace Engineering, University of Southern California

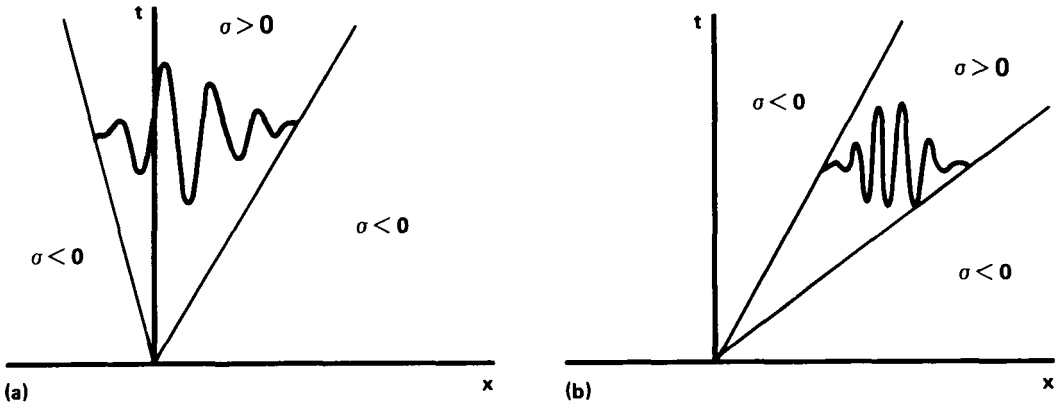

FIGURE 1. Sketch of a typical impulse response: *(a)* absolutely unstable flow; *(b)* convectively unstable flow.

small over a characteristic instability wavelength. One then says that the flow is *locally* absolutely unstable or *locally* convectively unstable at a given streamwise station. For instance, it has been demonstrated (Huerre & Monkewitz 1985) that the hyperbolic tangent mixing layer is convectively unstable for values of the velocity ratio $R = (U_1 - U_2)/(U_1 + U_2)$ smaller than one (*i.e.*, for coflowing streams), U_1 and U_2 being the respective velocities of each stream. Since this model is a good approximation to experimentally measured local mean velocity profiles, one may safely conclude that spatially-developing shear layers are locally convectively unstable everywhere: any initial vortical disturbance is advected downstream as it is amplified and the flow is extremely sensitive to external forcing (Ho & Huerre 1984). It is important to note that this locally convective behavior strictly pertains to *vortical* fluctuations in the shear zone and not to pressure fluctuations in the outer potential flow.

Since there is no region of absolute instability, one cannot have a self-sustained *global* response (*i.e.*, a finely tuned oscillation with the streamwise coordinate as an eigenfunction direction) involving temporally amplified upstream and downstream propagating *vorticity* waves (Chomaz *et al.* 1988). In the absence of a splitter plate, a downstream body, or a "non-transparent" outflow or inflow boundary, one therefore does not expect a self-sustained fluctuation field unless the flow is continuously forced from the outside.

3. Effects of Boundary Conditions on Spatially-developing Simulations

A two-dimensional numerical code of the spatial mixing layer developed by the first author was used to conduct the present investigation. The boundary conditions applied to the perturbation quantities are indicated on Figure 2. The reference length and velocity scales are the inflow vorticity thickness and the velocity difference, respectively. In all cases there was no external forcing at the inflow boundary and no splitter plate was inserted into the flow. At a velocity ratio $R = 2/3$ and for a computational domain of streamwise extent $Lx = 250$, one obtains throughout the flow a self-sustained noisy dynamical state characterized by a broad power

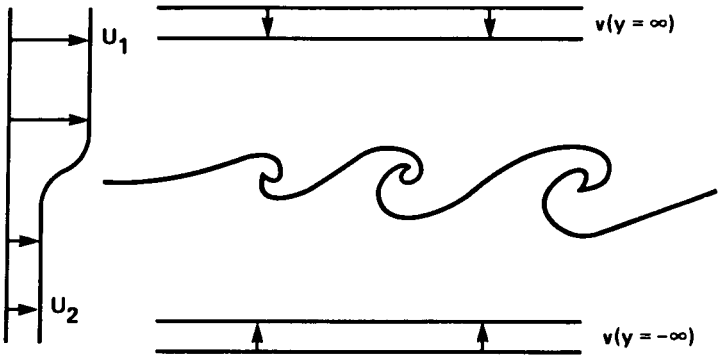

FIGURE 2. Geometry and boundary conditions.

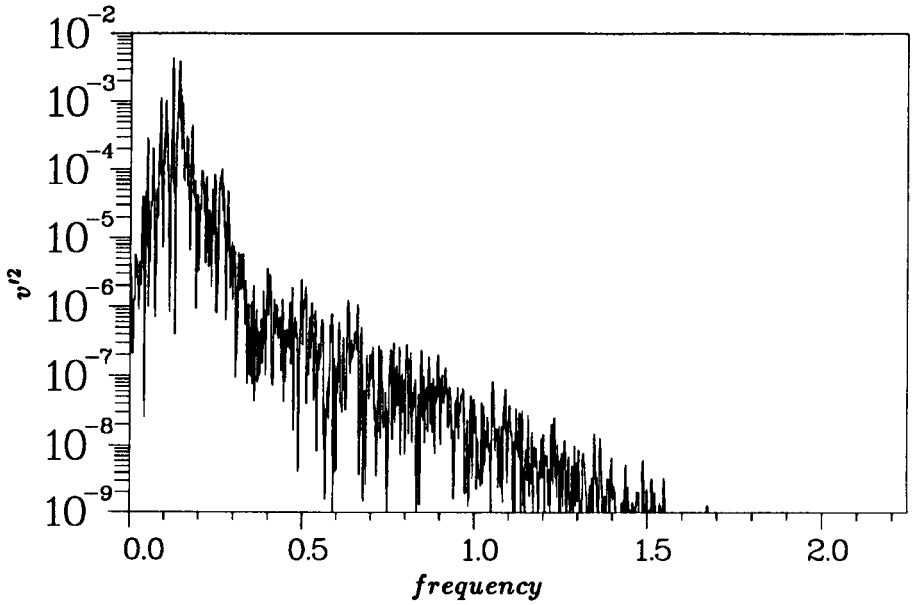

FIGURE 3. Power spectrum of v velocity at $x = 170$, $y = 0$.

spectrum, as shown in Figure 3. The spatial evolution of the vorticity field presents all the usual features of laboratory experiments, namely: spatial amplification of instability waves, roll-up, pairing of vortices, etc. The temporal behavior, however, appears to contradict the reasoning of the previous section: a convectively unstable flow should not be able to give rise to a "natural" self-excited state.

Time series of the cross-stream perturbation velocity v taken at different streamwise stations during the transient regime proved to be enlightening (see Figure 4). The discontinuity in slope generated at time $t = 0$ at the inflow boundary produces a wavepacket which propagates downstream. This discontinuity is induced by a mismatch between the initial conditions and the boundary condition at $x = 0$ (this

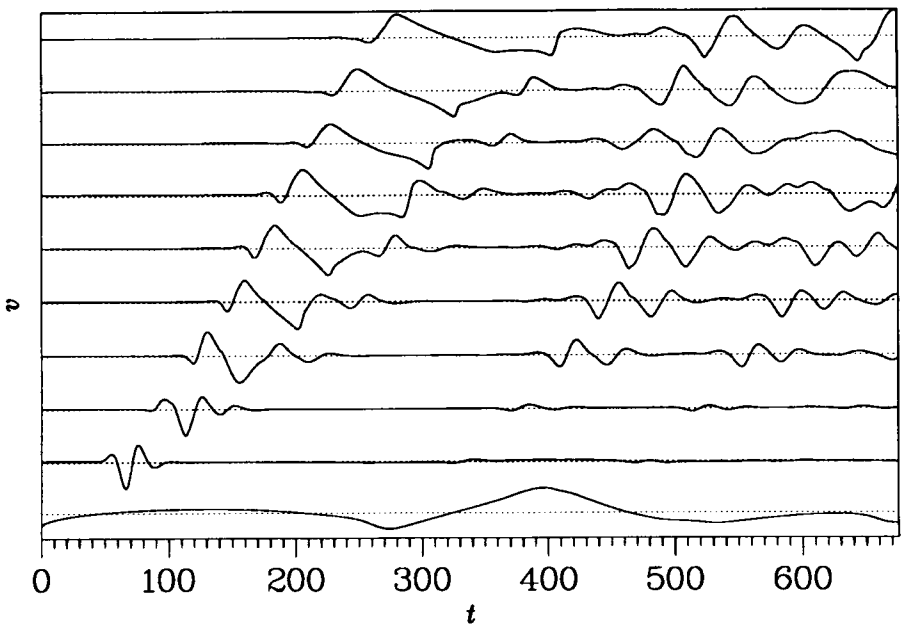

FIGURE 4. Time traces of v-velocity at $x = 1$, 50, 85, 115, 140, 160, 180, 200, 220, 249 (from bottom to top). Each trace is scaled with its maximum amplitude.

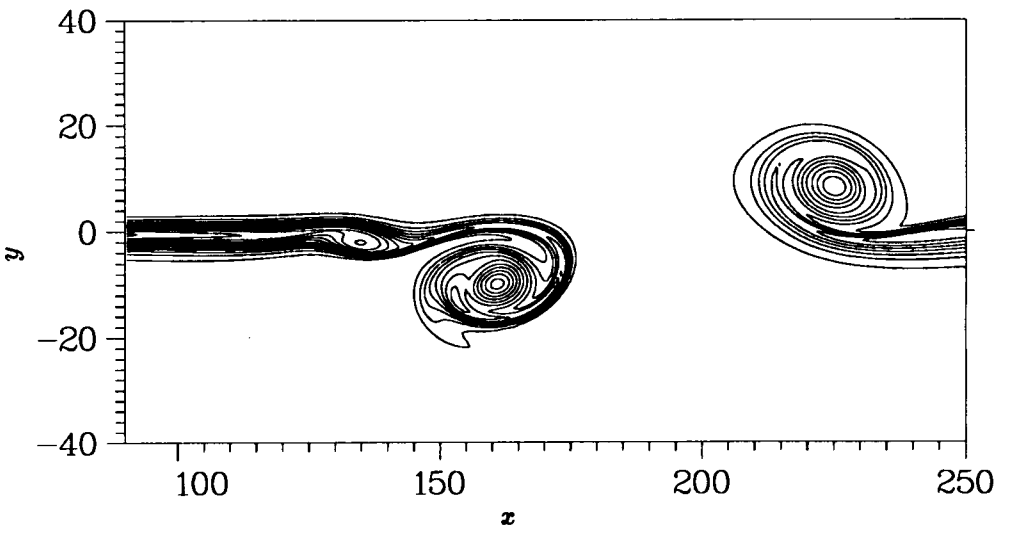

FIGURE 5. Contours of vorticity during the initial transient, showing the startup vortex pair.

appears to be unavoidable). The wavepacket is associated with the start-up vortex clearly seen in the downstream part of Figure 5. One can therefore conclude that the numerically generated velocity profile is indeed *convectively* unstable, the start-up transient being effectively a convolution of the initial state and the impulse response. Furthermore, one notes that, as soon as the wavepacket hits the downstream boundary, a sharp variation instantaneously takes place in the signal measured at the inflow. This local inhomogeneity in turn generates, after suitable filtering by the mean flow, a second wavepacket which also propagates downstream. It appears that the self-excited noisy state is induced by multiple reflections at the inflow and outflow boundaries of the computational domain. But temporally amplified vorticity waves cannot propagate upstream since the flow is convectively unstable!

Such is not the case for the pressure fluctuations prevailing outside the shear layer: Figure 6 presents statistical averages of various fluctuating variables plotted as a function of the cross-stream coordinate y. Two distinct regions are clearly in evidence: an exponential decay (linear on the semi-log plot) region followed by a much slower decay rate in the farfield region. The transition between the two regions is well-defined. The velocity in the second region might be associated with algebraically decaying pressure fluctuations generated by spatial inhomogeneities of the vorticity field due to modulations (Crighton & Huerre 1984) or pairing events (Gutmark & Ho 1985). Another likely candidate is the pressure field generated by multiple reflections at the inflow and outflow boundaries (strictly speaking, such a terminology is not legitimate: the potential flow is governed by an elliptic Poisson equation and information is transmitted instantaneously everywhere). Levels of constant mean-square v velocity are displayed in Figure 7. Levels are equally distributed on a log scale (two levels per decade). One observes a strong maximum at the outflow boundary, with equally separated contours in the downstream portion of the domain. Slower decay takes place in the upstream region, as indicated by increasing separation between neighboring contours. One may therefore infer that the v fluctuations in that region are due to pressure waves "radiating" towards the inflow boundary.

The following scenario emerges: the flow is locally convectively unstable from the point of view of vorticity fluctuations, but the global dynamics of the flow is dominated by a feedback loop (Laufer & Monkewitz 1980, Ho & Huerre 1984). The downstream branch consists of rotational instability waves rolling up into vortices. The interaction between the vortical structures and the downstream boundary then generates global irrotational pressure disturbances which are immediately transmitted to the inflow boundary. These are in turn converted into hydrodynamic instability waves by the inflow boundary condition. The noisy state is due to the relatively long streamwise extent of the computational domain which does not allow for stable periodic behavior. In a sense, the numerical experiment simulates a closed flow which, at this particular value of Lx, is in a highly chaotic dynamical state. This is consistent with a closer examination of Figure 3. The power spectrum is not just a continuous broadband one, but exhibits in addition closely spaced peaks.

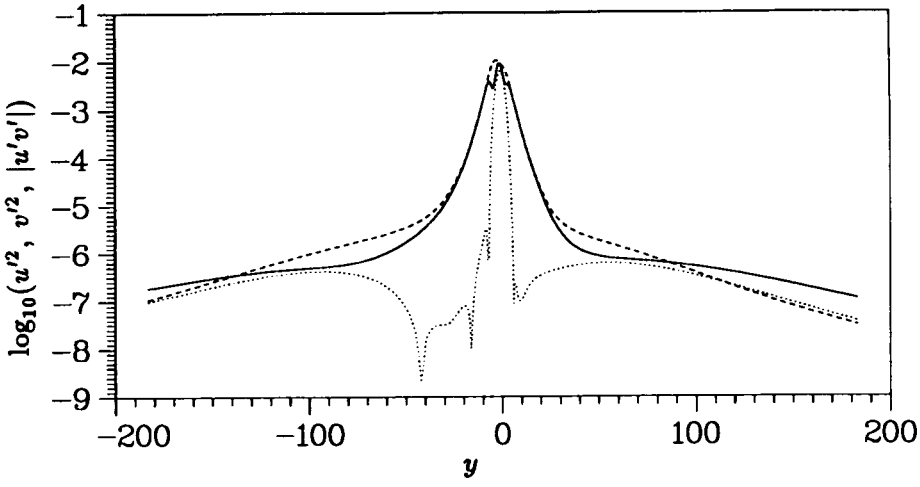

FIGURE 6. y-profiles of time-averaged statistics at $x = 125$: u'^2 (solid), v'^2 (dashed), $|u'v'|$ (dots).

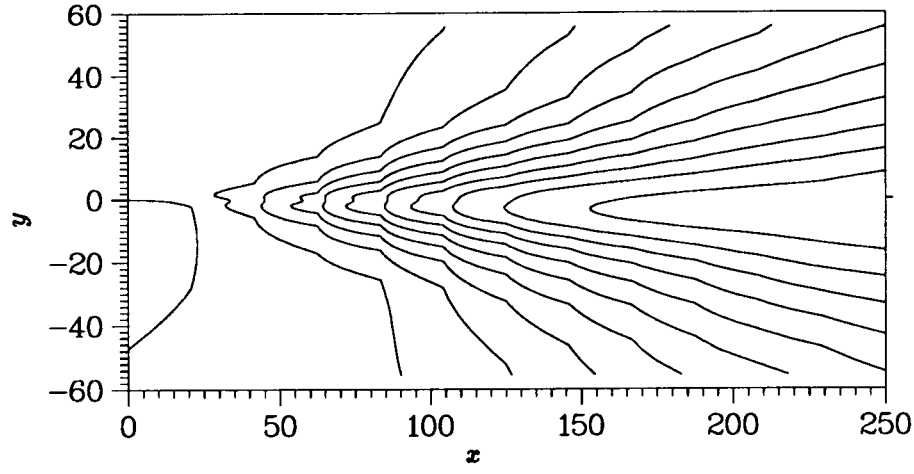

FIGURE 7. Contours of time-averaged v'^2.

Between frequencies 0.1 and 0.2 (for example) these peaks are equally spaced with the separation equal to the "box frequency", $(2\pi)\frac{1}{2}(U_1 + U_2)/Lx$. Thus the effect of the feedback appears directly in the spectrum.

The above scenario is further supported by the observed behavior of the system as the domain length Lx is varied. As mentioned previously, one sees a chaotic state when Lx is sufficiently large. For small Lx (*i.e.*, less than 100), the system approaches a steady state. For Lx not too much above 100, a periodic state is obtained (albeit after a long transient in some cases). Thus, one can think of Lx as a bifurcation parameter. Figure 8 shows the variation in amplitude of the fluctuation v velocity at two x locations as Lx increases from 100. The trend is consistent

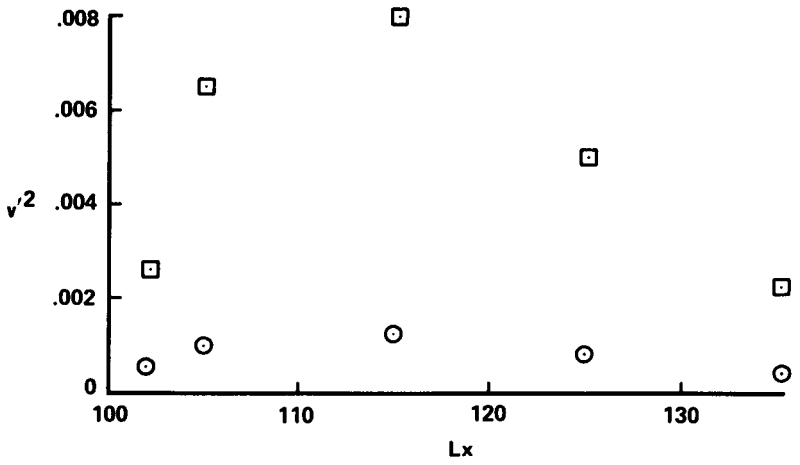

FIGURE 8. Maximum amplitude (in y) of v'^2 as a function of Lx at $x = 85$ (circles) and $x = 100$ (squares).

with a supercritical Hopf bifurcation from a steady state to a periodic orbit at approximately $Lx = 100$. A distinctive feature of all the periodic solutions obtained is that an exact integral number of instability wavelengths λ fit in the domain. For $102 \leq Lx \leq 125$, we found $\lambda = \frac{1}{4}Lx$, and for $Lx = 135$, $\lambda = \frac{1}{5}Lx$. Thus, the perturbations at the inflow and outflow boundaries are exactly in phase, indicating instantaneous communication through global pressure fluctuations. The decrease in amplitude for $Lx > 115$ is due to the largest fluctuations being associated with the outflow boundary (in these simulations, at most only one rollup is obtained). For sufficiently large Lx (in the chaotic regime), the fluctuation amplitudes at a given x become independent of Lx.

4. Finite Domains and Pressure Sources

The results of the previous section indicate that self-sustained oscillations are due to global pressure fluctuations being instantaneously transmitted between the inflow and outflow boundaries. In other words, the imposed boundary conditions do not correspond to those appropriate for an infinite (streamwise) domain. To cure this problem, one might try, in some way, to adapt the boundary conditions on the finite domain to simulate more accurately those of the infinite domain. We do not have an explicit scheme to suggest but only a very preliminary analysis.

For instance, we may consider the boundary-value problem

$$\nabla^2 p = Q, \qquad p = 0 \text{ on } S.$$

for the pressure p within a finite volume V bounded by a surface S. (Nuemann instead of Dirichlet boundary conditions may be imposed with little change in the following analysis). The source distribution $Q(\mathbf{x})$ is contained within V and takes the form

$$Q(\mathbf{x}) \equiv \frac{\partial^2(u_i u_j)}{\partial x_i \partial x_j}.$$

Let $G(\mathbf{x}|\mathbf{x}_0)$ denote the *free space* Green's function such that

$$\nabla^2 G = \delta(\mathbf{x} - \mathbf{x}_0).$$

The function $G(\mathbf{x}|\mathbf{x}_0)$ gives the pressure field generated by a point source located at $\mathbf{x}_0$ and "radiating" in free space. From Green's theorem, one may show that $p(\mathbf{x}, t)$ satisfies the *integral* equation

$$p(\mathbf{x},t) = \int_V G(\mathbf{x}|\mathbf{x}_0) Q(\mathbf{x}_0) dV_0 + \int_S \left[p(\mathbf{x}_0) \frac{dG}{dn_0}(\mathbf{x}|\mathbf{x}_0) - G(\mathbf{x}|\mathbf{x}_0) \frac{dp}{dn_0}(\mathbf{x}_0) \right] dS_0. \quad (1)$$

The volume integral corresponds to the pressure field in *free space* due to the source distribution Q within the field. The surface integral is associated with finite domain effects. Since $p = 0$ on S, only the pressure gradient dp/dn_0 remains. The surface integral is then the pseudo-sound field generated by a source distribution of strength $-dp/dn_0$ on the surface S. It is precisely this term that is responsible for the "reflections" observed in the numerical simulations. Whether active control methods can be used to cancel such surface integral terms remains to be determined. It might also be possible to obtain approximate expressions for these terms in the case of large computational domains. One must also point out that similar source distributions can also be obtained for the Navier-Stokes equations as derived in Ffowcs Williams & Hawkins (1969).

A possible use of equation (1) might involve minimizing the component of the pressure field at the inflow ($x = 0$) due to surface sources at the outflow ($x_0 = Lx$), by adjusting the outflow boundary conditions on u and v. If dp/dn_0 is known (from the u-momentum equation), then this will require an estimate of how p at the exit plane depends on the outflow velocity boundary conditions. Whether this can be done without actually solving the Poisson equation for pressure is not presently known.

Acknowledgments

We have benefitted from stimulating discussions with Chih-Ming Ho, Sanjiva Lele, Parviz Moin and Jim Riley. In addition to support of the C.T.R. Summer Program, P. Huerre would like to acknowledge support from a Joint NASA/USC Research Interchange. This work was done while J. Buell held a National Research Council-NASA Ames Research Associateship.

REFERENCES

BERS, A. 1975 in *Physique des Plasmas* (ed. C. DeWitt & J. Peyrand), pp. 117-213. New York: Gordon-Breach.

BRIGGS, R.J. 1964 Research Monograph No. 29. Cambridge, Mass.: M.I.T. Press.

CHOMAZ, J.M., HUERRE, P. & REDEKOPP, L.G. 1988 *Phys. Rev. Lett.* **60**, 25-28.

CRIGHTON, D.G. & HUERRE., P. 1984 AIAA Paper 84-2295.

FFOWCS WILLIAMS, J.E. & HAWKINGS, D.L. 1969 *Phil. Trans. R. Soc. Lond.* **A264**, 321-342.

GUTMARK, E. & HO, C.M. 1985 *AIAA J.* **23**, 354-358.

HO, C.M. & HUERRE, P. 1984 *Ann. Rev. Fluid Mech.* **16**, 365-424.

HUERRE, P. 1987 in *Instabilities and Nonequilibrium Structures* (ed. E. Tirapegui & D. Villaroel), pp. 141-177. Dordrecht: Reidel.

HUERRE, P. & MONKEWITZ, P.A. 1985 *J. Fluid Mech.* **159**, 151-168.

KOCH, W. 1985 *J. Sound and Vib.* **99**, 53-83.

LAUFER, J. & MONKEWITZ, P.A. 1980 AIAA Paper 80-0962.

MONKEWITZ, P.A. 1988 *Phys. Fluids* **31**, 999-1006.

Page intentionally left blank